Review Article

NUMERICAL INVESTIGATION OF THERMALLY COUPLED CATALYTIC MICROREACTORS USING COMPUTATIONAL FLUID DYNAMICS

JUNJIE CHEN*, LONGFEI YAN

Department of Energy and Power Engineering, School of Mechanical and Power Engineering, Henan Polytechnic University, Jiaozuo, Henan, China

Email: cjjmmm@163.com

ABSTRACT

Ammonia decomposition thermally coupled with methane catalytic combustion in catalytic microreactors for hydrogen production was studied numerically, using a two-dimensional computational fluid dynamics model. The effect of flow configuration on the operation characteristics was studied, and different performance measures were evaluated to assess the operability of the reactor. It was found that for a given flow rate of combustible mixture, the maximum power generated is determined by extinction at large decomposition stream flow rates, whereas material stability determines the lower power limit. Complete conversion of ammonia can be achieved in both flow configurations. A proper balance of the flow rates of the decomposition and combustion streams is crucial in achieving this. The two flow configurations were contrasted based on multiple performance criteria. For highly conductive materials, the co-current and counter-current flow configurations behave similarly in all performance measures. The counter-current flow configuration shows superior performance albeit in a very narrow operating regime of highly conductive materials and high ammonia flow rates, whereas the co-current flow configuration enables lower temperatures and a wider spectrum of materials to be used.

Keywords: Reactor model, Hydrogen production, Ammonia decomposition, Catalytic combustion, Flow configuration, Computational fluid dynamics

INTRODUCTION

Multifunctional reactors offers a useful framework for reactor selection and classification, which are reaction equipment in which one or more additional process functions such as heat, mass and momentum transport, or independent reactions are integrated [1]. They are widely used in industries as process intensification tools, making the process more efficient and compact and leading to large savings in the operational and capital costs. A multifunctional reactor can be used, for example, for coupling exothermic and endothermic reactions. In it, an exothermic reaction is used as the heat producing source to drive the endothermic reactions. The search for efficient new reactor concepts for coupling exothermic and endothermic reactions has been intensified in the last decade in an attempt to produce syngas in a cost-effective manner.

Coupling of strong endothermic reactions with heat exchange is often found in large-scale processes such as oxidative dehydrogenation, hydrocarbon cracking, and steam reforming. A heating medium or an exothermic reaction can provide the heat demand of the endothermic reaction at high temperatures. Three alternatives exist to combine the endothermic process and the heat supplied by an exothermic reaction namely direct coupling (directly coupled adiabatic reactor), regenerative coupling (reverse-flow reactor), and recuperative coupling (counter-current heat exchanger reactor, co-current heat exchanger reactor) [2]. In directly coupled adiabatic reactors, reactants for both endothermic and exothermic reactions are mixed and all reactions run in parallel, subject to a direct heat transfer within the reacting mixture, i.e., both reactions take place simultaneously in the same bed. This has been applied industrially in secondary methane steam reforming within the ammonia synthesis process and hydrogen cyanide synthesis, where the combustion of hydrogen-air mixture is used to produce in situ heat for the endothermic reactions. Other examples of its use are coupling of methane steam reforming with catalytic oxidation of methane in partial oxidation reactors, coupling of propane combustion and endothermic thermal cracking of propane to

propylene and ethylene, and in situ hydrogen combustion in oxidative dehydrogenations [3]. In reverse flow reactors, the exothermic and endothermic reactions occur periodically in the same catalyst bed. Here, the exothermic fuel combustion reaction takes place in the first half of the cycle. Then, in the next half cycle, the flow is reversed and the endothermic reaction takes place using the energy stored in the bed during the previous exothermic half cycle. During the exothermic cycle the fixed bed is heated and the stored heat is consumed in the next cycle when the endothermic process takes place cooling the fixed bed. Hence, the reverse flow reactors have to be operated in a dynamic fashion. The methane steam reforming coupled with methane catalytic combustion in reverse flow reactors has been widely studied [4]. One of the major concerns in the directly coupled adiabatic reactors and reverse flow reactors is that the catalyst used should preferably favor both exothermic and endothermic reactions or at the very least not get damaged by the exothermic reaction. Another constraint in these reactors is that the exothermic and endothermic reactions are carefully chosen so that the separation and purification of the products are minimized or avoided. For the directly coupled adiabatic reactors, bi-functional catalysts that promote both endothermic and exothermic reactions in the same temperature range are required [5]. If a mechanical mixture of two different catalysts is used heat transfer between them may limit conversion. For the reverse flow reactors, hot spots that can damage the catalyst and the reactor material can occur [6]. The above issues can be addressed by properly designed spatially segregated systems. Some of the above constraints can be circumvented in the recuperative reactors with either counter-current or co-current flow where the endothermic and exothermic reactions are separated in space. The benefits of such approach have been explained in the context of the catalytic plate reactor which is comprised of closely spaced catalytically coated metal plates [7]. The catalytic plate reactor effectively short-circuits heat transfer resistances between the reaction site and heating medium. The use of catalytic combustion to provide the heat required has various advantages [8]. It proceeds at

lower temperature than homogeneous combustion, which reduces the formation of nitrogen oxide. The operating window in terms of inlet fuel concentration is expanded. Lower operating temperature poses less constraint for the materials of construction. Since it is a flameless process, long radiation paths needed in conventional furnaces are replaced by channel dimensions of a few millimeters in the plate matrices, with an obvious impact on the reactor dimension.

The above recuperative or heat exchanger reactors offer several advantages over the directly coupled adiabatic reactors and the reverse flow reactors. Here, the products of the endothermic reaction are always separated from the combustion products. Since the exothermic side is spatially separated from the endothermic side, air can also be used for combustion instead of oxygen and the challenge of nitrogen separation from the product mixture does not exist. This in turn avoids the capital cost resulting from the installation of an oxygen separation unit and/or the operational cost resulting from compressing the air to the process pressure. Heat exchanger reactors offer other operational flexibilities since the operating parameters of exothermic and endothermic streams can be adjusted independently without affecting the other stream.

Hunter and McGuire are among the first to suggest the coupling of endothermic with exothermic reaction by means of indirect heat transfer [9]. They consider heat exchangers where catalytic combustion or other highly exothermic reaction is used as a heat source for an endothermic reaction. Ioannides and Verykios [10] explore another concept of integrating different reactions for synthesis gas production. The reactor consists of a ceramic tube in the inner and outer surface of which a metal catalyst film is deposited. A methane-oxygen feed enters into the tube and a large fraction of the heat generated on the wall by methane combustion is transported across the tube wall towards the outer catalyst film, where the endothermic reforming reactions take place. In this way, the temperature in the combustion region is controlled and hot spots are significantly reduced in magnitude. Venkataraman *et al*. [11] explore theoretically and experimentally the ethane dehydrogenation coupled with the methane catalytic combustion in the concentric tube flow configuration operating at high temperatures. Heat losses are reduced by adding multiple passes that enabled the hot combustion exhaust to preheat the inlet combustion gases. The reactor give better performance than a conventional steam cracker in terms of residence time and ethylene yield, and it offers considerable potential for coupling catalytic exothermic-catalytic endothermic reactions. The co-current flow pattern produces a more uniform temperature profile and give higher selectivity to ethylene. Polman *et al*. [12] achieve experimentally nearly complete conversions of combustion and reforming reactions, respectively, in a co-current plate reactor. Kolios *et al*. [13] study the process both experimentally and theoretically, mainly in counter-current configuration utilizing a ceramic honeycomb monolith with specially designed reactor heads. An optimal overlapping of the reaction regions is needed in order to control the reaction temperature. In countercurrent operation an essential feature for a successful solution is to raise the temperature of the exothermic reaction in the reaction region quickly above the temperature of the endothermic reaction in order to avoid back-transfer of heat within the main reaction region. A heat exchanging tubular reactor is developed and tested by Ismagilov *et al*. [14]. Methane combustion and steam reforming catalysts are incorporated within metal foams attached to the external and internal surfaces of a stainless-steel metal tube. By adding hydrogen in the combustible mixture, conversion of methane in the steam reforming section can be significantly increased.

In this study, a spatially segregated mode of the coupling of endothermic and exothermic reactions was investigated in parallel plate multifunctional microreactors, using a two-dimensional computational fluid dynamics model for co-current and counter-current flow configurations, where ammonia decomposition over ruthenium was coupled with methane catalytic combustion. The latter was chosen to enable high temperatures and complete conversion within short contact times while eliminating problems associated with catalyst deactivation. Furthermore, the effect of flow configuration on operation maps of coupled reactors using various

performance measures was explored. The objective of this study is to develop general design guidelines of integrated multifunctional microreactors.

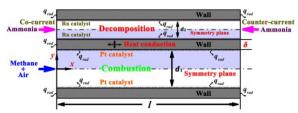## NUMERICAL MODELS

Geometric model

Fig. 1: Schematic diagram of the simulated parallel plate multifunctional microreactor with alternating combustion and decomposition channels.

The reaction system considered is coupling of the methane combustion and ammonia decomposition. An integrated parallel plate microreactor geometry is simulated. The combustion and decomposition reactions are carried out in alternate channels separated by walls, as shown schematically in Figure 1. The reactor length is 20.0 mm. The decomposition channel is 0.3 mm wide, the combustion channel is 0.6 mm wide, and the wall is 0.3 mm thick. The stoichiometric methane-air flow in the combustion channel is either co-current or counter-current with respect to the pure ammonia flow in the decomposition channel, which has ruthenium catalyst deposited on the channel walls. The ammonia decomposition reaction occurs at the catalytic channel wall resulting in hydrogen production. Unless otherwise stated, the methane-air inlet flow velocity is 0.8 m/s. Both the fluid streams enter the reactor at ambient temperature. Using the inherent symmetry of the geometry, only one-half of each channel and the connecting wall are simulated. The fluid flow and the heat and mass transfer equations are solved in the fluid phase and the energy balance is explicitly accounted for in the solid walls. The most common catalysts used for catalytic combustion of methane are supported precious metal catalysts. With platinum catalysts, the reaction order in oxygen tends towards zero, while the order in methane is usually about unity. The activation energy depends on the precious metal and reaction conditions.

Mathematical model

The insights gained from the gas-phase micro-combustors are not necessarily applicable to the catalytic systems studied in this work. For example, temperatures in gas-phase combustion are too high in comparison to those in catalytic combustion. Furthermore, while gaseous radicals are typically quenched on walls, causing flame extinction, catalysts serve mainly to form radicals that drive surface chemistry. Heat transfer is also different. For gas-phase micro-combustors, heat transfer of the heat generated in the gas phase to the walls can be slow in comparison to the chemistry time scale. On the other hand, the heat is liberated on the wall in the catalytic micro-combustors, accelerating heat transfer within the walls. As a result of such differences, a model incorporating catalytic combustion is developed. The following assumptions are made in the development of the model: the resistance across the gas-solid film for heat and mass transfer is assumed to be negligible, axial mass and heat dispersions are neglected, a constant heat transfer coefficient has been assumed along the length of the reactor, the total pressure of the system is constant.

The value of Knudsen number is first estimated, and it has been found that the characteristic scale of channel is still notably larger than the mean free path of gas molecular. Consequently, fluids can be reasonably treated as continuums and the Navier-Stokes equations are still applicable to the present work. A laminar flow is employed in each channel because the Reynolds number (Re) based on the incoming properties and the channel hydraulic diameters is less than 480. Atmospheric pressure is considered in all simulations. A two-dimensional steady state model is employed using the commercial computational fluid dynamics software package ANSYS

FLUENT® Release 6.3 incorporates with the detailed homogeneous and heterogeneous reaction schemes in CHEMKIN and Surface-CHEMKIN format to solve the steady state continuity, momentum, energy, and species equations with appropriate boundary conditions. The species diffusion velocities are computed using a mixture-average transport model including thermal diffusion. At the vertical wall faces, both convective and radiative boundary conditions are applied to compute external heat losses. Since the heat recirculation within the wall profoundly affects the combustion stability, the heat conduction within the walls is considered. Radiation exchange between the discretized inner surface elements, as well as between the surface elements themselves and the inlet and outlet channel enclosures is accounted for by the net radiation method for diffuse-gray areas. Concerning the species boundary conditions, the flux of a gas-phase species at the surface is equal to its net rate of consumption due to interfacial reactions. The interfacial reactions are define as the reactions which include at least one surface species. For a surface species, at steady state the net reaction rate is equal to zero. Finally, the coverage of vacancies is computed from an overall balance on catalyst sites.

Chemical kinetics

A two-dimensional numerical model is used for both the gas and the solid, which includes elementary homogeneous and heterogeneous reaction mechanisms, detailed transport, heat conduction in the solid, and surface radiative heat transfer. For the catalytic combustion of methane-air mixtures over platinum, the detailed heterogeneous reaction scheme of Deutschmann *et al*. [15] is employed, including 24 elementary reactions, 11 surface and 9 gaseous species. A surface site density $\Gamma_{Pt} = 2.72 \times 10^{-9}$ mol/cm^2 is used for the platinum catalyst. Even though gas-phase reactions are taken into account, it has been shown that the reactor performance is not affected by gas-phase reactions. Thus, gas-phase chemistry is not discussed further here. For the ammonia decomposition over ruthenium, the detailed heterogeneous reaction scheme of Deshmukh *et al*. [16] is employed. This scheme has been used in computational fluid dynamics simulations of microreactors, and good agreement with experimental data can be observed. A surface site density $\Gamma_{Ni} = 2.90 \times 10^{-9}$ mol/cm^2 is used for the ruthenium catalyst. The computational tool DETCHEM is employed to treat the problem numerically. Gaseous and surface thermodynamic data are included in the provided schemes. Mixture-average diffusion coefficients are used in conjunction with the CHEMKIN transport database. Gas-phase and surface reaction rates were evaluated with CHEMKIN and Surface-CHEMKIN, respectively.

Computation scheme

The thermal conductivity, viscosity, and specific heat are computed using a mass fraction weighted average of the species properties. The species specific heats are computed using a piecewise polynomial fit of the temperature [17]. The species viscosities and thermal conductivity are determined from kinetic theory. Multicomponent diffusion is considered in this system, where the binary diffusion coefficients are determined from kinetic theory [18]. For the solid wall, a constant specific heat and an isotropic thermal conductivity are specified. Given that material thermal conductivity varies with temperature and more importantly with the material chosen, computations are carried out over a wide range of wall thermal conductivities. An adaptive meshing scheme is used for the discretization of the differential equations. The computational mesh is initialized with 200 axial nodes, 80 radial nodes for the combustion channel and the wall sections, and 60 radial nodes for the reforming channel. This initial mesh is adapted and refined during a computation to increase the accuracy of the solution in regions of high gradients. Specifically, additional nodes are introduced to refine the mesh using the tools built in the computational software so that the normalized gradients in temperature and species between adjacent cells are lower than 10^{-6}. Adaptation is performed if the solution has not converged after about 10^6 iterations or when the residuals are around 10^{-6}. This last threshold, while not optimized, is meant to strike a balance between cost and probability for convergence. Specifically, mesh refinement before achieving complete convergence reduces the computational

effort, but a too early refinement, i.e., in a few iterations, may lead to refinement in wrong regions. After mesh refinement, a total of 80000-600000 nodes are used. Such an adaptive meshing strategy, starting with a relatively coarse initial mesh followed by refinement in regions of large gradients, achieves an adequate balance between accuracy and computational effort.

Symmetry boundary condition is applied at the centerline of both channels, implying a zero normal velocity and zero normal gradients of all variables [19]. No-slip boundary condition is employed at each wall-fluid interface. Danckwerts boundary conditions are used for the temperatures and species at the inlets to better mimic experimental conditions [20]. The reactor exits are held at a fixed atmospheric pressure and the normal gradients of species and temperature, with respect to the direction of the flow, are set to zero. Continuity in temperature and heat flux is employed at the fluid-solid interfaces. It should be noted that neither heat-transfer nor mass-transfer correlations are employed since detailed transport within the solid and fluid phases is explicitly accounted for. The full problem is solved through a segregated solver using an under-relaxation method. Convergence of the computational fluid dynamics simulation is judged based on the residuals of all governing equations to be less than 10^{-6}. Coupling of the heat equation within the walls and the reacting flow equations makes the problem stiff due to the disparity in thermal conductivity between the gases and the walls. Natural parameter continuation is employed to study the effect of various operating parameters.

OPERATING LINE

Important operating lines in multifunctional reactors include material stability and maximum power output. In this study, an arbitrary maximum temperature of 1500 K is proposed as the material stability limit, i.e., catalyst and wall temperatures higher this value are deemed detrimental to the reactor, given the fact that lower reactor temperatures are essential for the stability of construction materials and catalyst employed in the ammonia decomposition channel. The choice of the temperature threshold defined here stems from similar temperatures observed in short contact time reactors, in which noble metal catalysts have been found to be stable up to temperatures of 1500 K [21]. Furthermore, supported ruthenium catalysts have been found to be stable for periods of hundreds of hours tested [22]. The material stability determines the lower power limit for a given combustible mixture flow velocity, caused by the high temperatures generated at low ammonia flow velocities. On the other hand, the maximum power output corresponds to the maximum hydrogen yield, which is in the incomplete ammonia conversion region [23]. This operating line is determined from the ammonia conversion and the combustible mixture flow velocity, caused by the trade-off between higher flow velocity and lower ammonia conversion [24]. Coupling of methane catalytic combustion with ammonia decomposition has been simulated for both co-current and counter-current operation, using identical parameters of the mathematical model. Consequently, a direct comparison between the reactor behavior and performance under different flow configurations can be made.
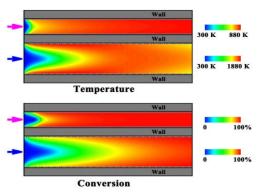
OPERATION CHARACTERISTICS

Fig. 2: Temperature and conversion contours for a typical set of operating parameters.

Here, the operation characteristics of co-currently coupled micro-devices are presented. To obtain an ignited stable solution, initial calculations are performed with a highly conductive wall to achieve better heat recirculation and a low ammonia flow rate to minimize heat removal from the reforming channel. The methane-air inlet flow velocity is 0.8 m/s, and the ammonia inlet flow velocity is 0.6 m/s. The wall is assumed to be made of a highly conductive material with a thermal conductivity of 80.0 W/m·K. Figure 2 shows the temperature and conversion contours for a typical set of operating parameters. The results demonstrate self-sustained operation within the micro-device with nearly complete conversion of methane and ammonia. The high wall temperatures near the inlets pre-heat the incoming flows to ignition. The wall causes heat recirculation from downstream of the combustion region to the entrance. Flames are stabilized at the centerline of the combustion channel near the entrance. Despite the small scales, there are significant species and temperature gradients within the fluid near the reaction region. The co-current configuration allows overlap of the reaction regions localizing the gradients in temperature near the entrances. Reactions are completed within a few millimeters from the entrance. Downstream of the reaction regions the device is nearly isothermal because of fast heat transfer caused by the small scales of the reactor. The high conductivity of the material leads to a nearly isothermal wall. In these integrated micro-devices, the role of the wall is to serve as a heat recirculating medium. Catalytic combustion generates energy that is transferred relatively fast to the catalytic walls. The fast conducting wall enables backward heat transfer toward the entrance of the methane-air mixture to cause ignition of the combustible mixture; i.e., by recirculating energy, the wall serves as an ignition source. Similarly, the ammonia stream is heated by the hot wall and reaches the wall temperature near its entrance, a feature attributed to the fast heat transfer between the gas and the surface for such a narrow channel. This heat transfer from the ammonia stream to the combustion stream renders the stability of the coupled reactors higher than that of combustors alone.
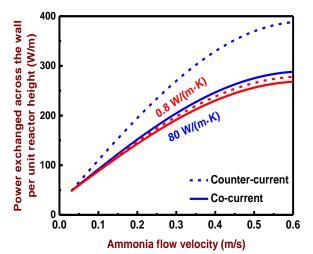
POWER EXCHANGED

Fig. 3: Effect of ammonia flow velocity on the power exchanged across the wall per unit reactor height for different wall thermal conductivities.

Figure 3 shows the effect of ammonia flow velocity on the power exchanged across the wall per unit reactor height for different wall thermal conductivities. Previously, the critical power removed at extinction has been used as a stability criterion for gas-phase micro-combustors [25]. The power exchanged across the wall is an important performance measure since a primary objective of a multifunctional reactor is to maximize the heat exchange between the two reaction regions. The end points of each curve at high ammonia flow rates correspond to the critical power exchanged prior to extinction. In the co-current flow configuration, the power exchanged is practically independent of the material chosen. Additionally, a strong dependence of the power transferred on the

wall thermal conductivity can be observed in the counter-current flow configuration, especially at high ammonia flow rates. For highly conductive materials, corresponding to metals and high conductivity ceramics, the powers exchanged in the two flow configurations become practically equal, where the time-scale of axial heat conduction is so short that heat transfer is independent of the flow configuration. At the other extreme of low wall thermal conductivity, the time-scale of transverse heat conduction becomes larger than the residence time rendering the effect of flow configuration small. However, for moderate wall thermal conductivities, there is a competition between the flow residence time and heat conduction time-scale, and hence the flow configuration plays an important role in heat exchange. Specifically, for moderate conductive materials, the power exchanged in the counter-current flow configuration is larger. Materials in this conductivity range have previously been used for the fabrication of micro-combustors [26] and have been reported to be most stable to heat losses [27]. Consequently, although the counter-current flow configuration can achieve better performance for moderate wall thermal conductivities, the two flow configurations exhibit nearly identical reactor performance at the extremes of material conductivity range in terms of the power exchanged.
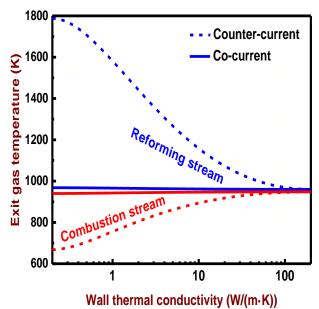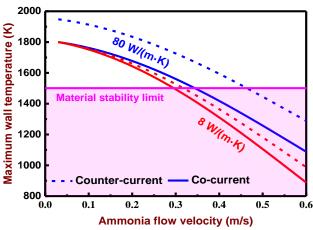
EXIT GAS TEMPERATURE

Fig. 4: Effect of wall thermal conductivity on the exit gas temperatures.

Figure 4 shows the effect of wall thermal conductivity on the exit gas temperatures. The ammonia inlet flow velocity is 0.8 m/s. In the counter-current flow configuration, the larger power exchanged comes at the expense of higher exit temperature of the decomposition stream, larger maximum wall temperature, because the decomposition stream flows past the hot combustion region, and a lower combustion stream exit temperature. High temperatures of the decomposition stream are undesirable for proton exchange membrane fuel cell applications for which the stream has to be cooled down to about 360 K [28]. Note that the proton exchange membrane fuel cell is a promising alternative power source for various applications in portable power device, vehicles, and stationary power plants [29]. Consequently, a comparison in terms of the critical power exchanged may be misleading and hence not a good reactor performance criterion for integrated systems producing hydrogen. These numerical results represent the rather expected outcome that optimizing individual components, e.g., a combustor and a reformer, is not necessarily a good strategy for developing design principles for coupled reactors.

EFFECT OF WALL THERMAL CONDUCTIVITY

Fig. 5: Effect of wall thermal conductivity on the maximum wall temperature at different ammonia inlet flow velocities. The material stability limit is represented by the shaded region.
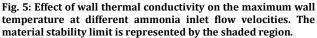
Figure 5 shows the of wall thermal conductivity on the maximum wall temperature at different ammonia inlet flow velocities. The wall thermal conductivity is an important parameter which determines the reactor stability. For highly conductive materials, the temperature profiles of the two flow configurations are nearly identical. The high wall thermal conductivity implies rapid heat conduction that leads to nearly isothermal wall temperatures. In this case, the time-scale of wall heat conduction is much smaller than the residence time rendering the effect of flow configuration secondary. However, with the decrease of wall thermal conductivity, differences between the two flow configurations emerge. In the counter-current flow configuration, the heat generation and heat removal are separated by the length of the reactor, and a low wall thermal conductivity implies slow heat transfer leading to very hot walls near the combustion region. In addition, significant temperature gradients may occur within the wall. Almost identical behavior of the two flow configurations is observed for high thermal conductivity materials. The maximum temperature of reactors in the co-current flow configuration is nearly independent of wall thermal conductivity, whereas reactors in the counter-current flow configuration exhibit very high wall temperatures at lower wall thermal conductivities. The shaded region demarcates the operating regime of allowable reactor temperatures. Operation in the co-current flow configuration allows a wider choice of materials and leads to lower reactor temperatures than that in the counter-current flow configuration.
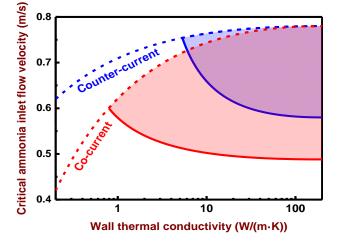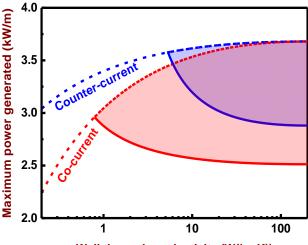
HYDROGEN PRODUCTION

Fig. 6: Effect of wall thermal conductivity on the critical ammonia inlet flow velocity. The shaded region represents the operating regime delimited by extinction and material stability.

Figure 6 shows the effect of wall thermal conductivity on the critical ammonia inlet flow velocity. The critical ammonia inlet flow velocity corresponds to extinction. The hydrogen flow rate is perhaps the most important performance measure of an integrated reactor. The hydrogen flow rate depends not only on the ammonia flow rate but also on the ammonia conversion. For a given wall thermal conductivity, any ammonia inlet flow velocity above the critical one, i.e., above the line connecting the points cannot be self-sustained. Consequently, operation is limited below the line of each flow configuration. Larger wall thermal conductivities lead to increased heat recirculation and hence aid in stabilizing higher ammonia flow rates, irrespective of the flow configuration. The overlap of reaction regions in the co-current flow configuration leads to diminished stability of the reactor, i.e., lower maximum ammonia flow velocities, especially for highly insulating materials. However, the difference in stability between the two flow configurations becomes less pronounced for highly conductive materials. Given that low ammonia flow rates lead to high wall temperatures, the shaded areas indicate a coarse operating regime of realizable flows and wall materials. The upper boundary of flow is determined from extinction, whereas the lower boundary of flow and wall thermal conductivity from the material stability limit. The materials limit criterion renders the counter-current flow configuration only slightly better for a narrow range of materials. It is clear that the co-current flow configuration allows a wider choice of wall materials.

MAXIMUM POWER GENERATED

Fig. 7: Effect of wall thermal conductivity on the maximum power generated based on the hydrogen produced. The shaded region represents the operating regime delimited by extinction and material stability.

Figure 7 shows the effect of wall thermal conductivity on the maximum power generated based on the hydrogen produced. The maximum power generated corresponds to the maximum hydrogen yield. Depending on the overall process flow sheet, operation with the maximum power generated may be desirable. The maximum power generated accounts for both the critical ammonia flow rate and the ammonia conversion, assuming 100% fuel cell efficiency. The shaded region demarcates again the operating regime delimited by extinction and material stability. Due to the high conversions under reasonable operating conditions, the similar features of the critical ammonia inlet flow velocity can be obtained. The counter-current operation is slightly better in a narrow operating regime. The co-current flow configuration allows a wider choice of fabrication materials and catalysts.

OPERATION MAP

In order to guide the design of integrated reactors based on a projected power requirement, operation maps are presented. While

these operation maps clearly pertain to the specific fuels and to parallel plate geometries of fixed dimensions, the approach employed herein is general and similar findings can be expected for other multifunctional micro-chemical devices. In all computations, a 100% fuel cell efficiency is assumed, given that a lower efficiency would scale the results exactly proportionally. Based on the discussion above, only a narrow range of powers can be achieved for a fixed methane-air flow rate.
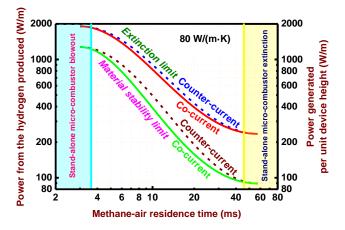

Fig. 8: Operation map indicating the power generated based on the hydrogen produced as a function of methane-air residence time. The vertical shaded areas represent those for a stand-alone micro-combustor.

The minimum power is determined from the lowest allowable ammonia flow rate that in turn is dictated by the material limit set at 1500 K. The maximum power corresponds to the critical value prior to extinction. The minimum power generated corresponds to the co-current flow configuration, whereas the maximum power generated corresponds to the counter-current flow configuration at high wall thermal conductivities. Powers outside this range cannot be achieved irrespective of the flow configuration or wall material chosen. One could envisage a "scale-out" type of approach [30], using multiple units in parallel, to achieve higher powers or changing the reactor dimensions to enable lower powers [31], while keeping the residence time constant [32]. It should be noted that the computed powers are dependent on the choice of fuel. However, given a single reactor consisting of two channels only with fixed channel length, operation outside this power range without changing the fuel implies varying the methane-air flow rates.

The fuel-air residence times in micro-combustors have been found to be restricted to a finite operating regime for self-sustained combustion [33]. Combustion stability plays an important part in reactor performance [34]. Very fast fuel-air flows cause blowout [35], given that the residence time is not long enough for self-sustained operation to be possible [36]; in contrast, very slow flows lead to extinction [37], since not enough heat is produced to keep up with the heat loss to the surroundings [38]. A two parameter continuation is used to track the power generation as a function of the ammonia flow rate for various methane-air residence times. Figure 8 shows the operation map indicating the power generated based on the hydrogen produced as a function of methane-air residence time. The shaded vertical rectangles provide an idea of the residence time limits. The limits of the operating regime depend on the wall material and the choice of flow configuration. High wall thermal conductivity represents the maximum power produced and also leads to an equivalent performance of the two flow configurations. Consequently, the counter-current flow configuration with a high wall thermal conductivity of 80 W/(m·K) is chosen for the majority of runs and computational fluid dynamics simulations are performed for different methane-air residence times. A narrow operating regime is achieved, as indicated by the cross-hatched area. For both flow configurations and all methane-air residence times, an upper bound for the power is caused by the critical ammonia inlet flow velocity, whereas the lower bound

depicts the material limit in terms of the reactor temperature. A balance between the methane-air and ammonia flow rates is crucial in enabling self-sustained operation of coupled reactors. Stable operation outside the methane-air residence time regime predicted by computational fluid dynamics simulations of the stand-alone micro-combustor is also an evidence of the enhanced stability of the integrated reactor. The power generation plots can be used as a guide in designing integrate reactors. One can select a desired power, and trace it to the operating regime to estimate the required methane-air residence time.

CONCLUSION

In this study, the operation of coupled microreactors was explored in a parallel plate device, with alternating exothermic and endothermic reaction channels separated by a wall. The catalytic combustion of methane-air mixtures over platinum as a heat source and ammonia decomposition over ruthenium as an endothermic reaction were chosen. Computations were carried out to develop general design guidelines of integrated multifunctional reactors, using a two-dimensional computational fluid dynamics model that included detailed chemistry and transport. The co-current and counter-current flow configurations were contrasted in terms of various performance criteria including reactor temperatures, exit gas temperatures, maximum power exchanged, and hydrogen production achieved. For any combustible flow rate, the operating regime of the reactor is delimited by extinction caused from fast ammonia flows as well as by material stability, in terms of reasonable reactor temperatures, at sufficiently slow ammonia flows.

The co-current and counter-current flow configurations behave similarly in all performance measures for highly conductive materials. This is simply because the high wall thermal conductivity coupled with small reactor scales renders the operation nearly isothermal. The counter-current flow configuration shows superior performance albeit in a very narrow operating regime of highly conductive materials and high ammonia flow rates, whereas the co-current flow configuration enables lower temperatures and a wider spectrum of materials to be used. Since this advantage of the counter-current flow configuration is only slight, the co-current flow configuration should be preferred for actual reactors.

The catalytic combustion of methane-air mixtures leads to a relatively narrow range of balanced flow rates in order to prevent material stability and avoid extinction issues; meanwhile it can lead to high temperatures and drive ammonia decomposition to completion in milliseconds. In order to broaden the operation regime, future work will explore the use of alternative coupling modes and chemistries.

REFERENCES

1. K.R. Westerterp. Multifunctional reactors. *Chemical Engineering Science*, Volume 47, Issues 9-11, 8 June 1992, Pages 2195-2206.
2. D.W. Agar. Multifunctional reactors: Old preconceptions and new dimensions. *Chemical Engineering Science*, Volume 54, Issue 10, May 1999, Pages 1299-1305.
3. J.D. Holladay and Y. Wang. A review of recent advances in numerical simulations of microscale fuel processor for hydrogen production. *Journal of Power Sources*, Volume 282, 15 May 2015, Pages 602-621.
4. Qi, B. Peppley, and K. Karan. Integrated fuel processors for fuel cell application: A review. *Fuel Processing Technology*, Volume 88, Issue 1, January 2007, Pages 3-22.
5. V.R. Choudhary, V.H. Rane, and A.M. Rajput. High-temperature catalytic oxidative conversion of propane to propylene and ethylene involving coupling of exothermic and endothermic.
6. reactions. *Industrial & Engineering Chemistry Research*, Volume 39, Issue 4, 2000, Pages 904-908.

7. A.M. De Groote and G.F. Froment. Simulation of the catalytic partial oxidation of methane to synthesis gas. *Applied Catalysis A: General*, Volume 138, Issue 2, 9 May 1996, Pages 245-264.

8. G. Kolb. Review: Microstructured reactors for distributed and renewable production of fuels and electrical energy. *Chemical Engineering and Processing: Process Intensification*, Volume 65, March 2013, Pages 1-44.

9. G.D. Stefanidis and D.G. Vlachos. Intensification of steam reforming of natural gas: Choosing combustible fuel and reforming catalyst. *Chemical Engineering Science*, Volume 65, Issue 1, 1 January 2010, Pages 398-404.

10. M. Zanfir and A. Gavriilidis. Catalytic combustion assisted methane steam reforming in a catalytic plate reactor. *Chemical Engineering Science*, Volume 58, Issue 17, September 2003, Pages 3947-3960.

11. T. Ioannides and X.E. Verykios. Development of a novel heat-integrated wall reactor for the partial oxidation of methane to synthesis gas. *Catalysis Today*, Volume 46, Issues 2-3, 16 November 1998, Pages 71-81.

12. K. Venkataraman, J.M. Redenius, and L.D. Schmidt. Millisecond catalytic wall reactors: dehydrogenation of ethane. *Chemical Engineering Science*, Volume 57, Issue 13, July 2002, Pages 2335-2343.

13. E.A. Polman, J.M. Der Kinderen, and F.M.A. Thuis. Novel compact steam reformer for fuel cells with heat generation by catalytic combustion augmented by induction heating. *Catalysis Today*, Volume 47, Issues 1-4, 1 January 1999, Pages 347-351.

14. G. Kolios, J. Frauhammer, and G. Eigenberger. Efficient reactor concepts for coupling of endothermic and exothermic reactions. *Chemical Engineering Science*, Volume 57, Issue 9, May 2002, Pages 1505-1510.

15. Z.R. Ismagilov, V.V. Pushkarev, Y.O. Podyacheva, N.A. Koryabkina, and H. Veringa. A catalytic heat-exchanging tubular reactor for combining of high temperature exothermic and endothermic reactions. *Chemical Engineering Journal*, Volume 82, Issues 1-3, 15 March 2001, Pages 355-360.

16. O. Deutschmann, L.I. Maier, U. Riedel, A.H. Stroemman, and R.W. Dibble. Hydrogen assisted catalytic combustion of methane on platinum. *Catalysis Today*, Volume 59, Issues 1-2, 10 June 2000, Pages 141-150.

17. S.R. Deshmukh, A.B. Mhadeshwar, and D.G. Vlachos. Microreactor modeling for hydrogen production from ammonia decomposition on ruthenium. *Industrial & Engineering Chemistry Research*, Volume 43, Issue 12, 2004, Pages 2986-2999.

18. D.G. Norton, E. D. Wetzel, and D.G. Vlachos. Fabrication of single-channel catalytic microburners: Effect of confinement on the oxidation of hydrogen/air mixtures. *Industrial & Engineering Chemistry Research*, Volume 43, Issue 16, 2004, Pages 4833-4840.

19. D.G. Norton, E. D. Wetzel, and D.G. Vlachos. Thermal management in catalytic microreactors. *Industrial & Engineering Chemistry Research*, Volume 45, Issue 1, 2006, Pages 76-84.

20. R. Sui and J. Mantzaras. Combustion stability and hetero-/homogeneous chemistry interactions for fuel-lean hydrogen/air mixtures in platinum-coated microchannels. *Combustion and Flame*, Volume 173, November 2016, Pages 370-386.

21. R. Sui, N.I. Prasianakis, J. Mantzaras, N. Mallya, J. Theile, D. Lagrange, and M. Friess. An experimental and numerical investigation of the combustion and heat transfer characteristics of hydrogen-fueled catalytic microreactors. *Chemical Engineering Science*, Volume 141, 17 February 2016, Pages 214-230.

22. P.M. Torniainen, X. Chu, and L.D. Schmidt. Comparison of monolith-supported metals for the direct oxidation of methane to syngas. *Journal of Catalysis*, Volume 146, Issue 1, March 1994, Pages 1-10.

23. Berman, R.K. Karn, and M. Epstein. Kinetics of steam reforming of methane on Ru/Al_2O_3 catalyst promoted with Mn oxides. *Applied Catalysis A: General*, Volume 282, Issues 1-2, 30 March 2005, Pages 73-83.

24. S.R. Deshmukh and D.G. Vlachos. Effect of flow configuration on the operation of coupled combustor/reformer microdevices for hydrogen production. *Chemical Engineering Science*, Volume 60, Issue 21, 2005, Pages 5718-5728.

25. S.R. Deshmukh and D.G. Vlachos. CFD Simulations of coupled, countercurrent combustor/reformer microdevices for hydrogen production. *Industrial & Engineering Chemistry Research*, Volume 44, Issue 14, 2005, Pages 4982-4992.

26. J.A. Federici and D.G. Vlachos. A computational fluid dynamics study of propane/air microflame stability in a heat recirculation reactor. *Combustion and Flame*, Volume 153, Issues 1-2, April 2008, Pages 258-269.

27. C.M. Miesse, R.I. Masel, C.D. Jensen, M.A. Shannon, and M. Short. Submillimeter-scale combustion. *AIChE Journal*, Volume 50, Issue 12, 2004, Pages 3206-3214.

28. J.A. Federici, E.D. Wetzel, B.R. Geil, and D.G. Vlachos. Single channel and heat recirculation catalytic microburners: An experimental and computational fluid dynamics study. *Proceedings of the Combustion Institute*, Volume 32, Issue 2, 2009, Pages 3011-3018.

29. N. Djilali. Computational modelling of polymer electrolyte membrane (PEM) fuel cells: Challenges and opportunities. *Energy*, Volume 32, Issue 4, 2007, Pages 269-280.

30. H.-W. Wu. A review of recent development: Transport and performance modeling of PEM fuel cells. *Applied Energy*, Volume 165, 2016, Pages 81-106.

31. M.S. Mettler, G.D. Stefanidis, and D.G. Vlachos. Enhancing stability in parallel plate microreactor stacks for syngas production. *Chemical Engineering Science*, Volume 66, Issue 6, 2011, Pages 1051-1059.

32. G.D. Stefanidis and D.G. Vlachos. Millisecond methane steam reforming via process and catalyst intensification. *Chemical Engineering & Technology*, Volume 31, Issue 8, 2008, Pages 1201-1209.

33. G.D. Stefanidis and D.G. Vlachos. High vs. low temperature reforming for hydrogen production via microtechnology. *Chemical Engineering Science*, Volume 64, Issue 23, 2009, Pages 4856-4865.

34. J. Wan, A. Fan, and H. Yao. Effect of the length of a plate flame holder on flame blowout limit in a micro-combustor with preheating channels. *Combustion and Flame*, Volume 170, 2016, Pages 53-62.

35. D.G. Norton and D.G. Vlachos. Combustion characteristics and flame stability at the microscale: a CFD study of premixed methane/air mixtures. *Chemical Engineering Science*, Volume 58, Issue 21, November 2003, Pages 4871-4882.

36. D.G. Norton and D.G. Vlachos. A CFD study of propane/air microflame stability. *Combustion and Flame*, Volume 138, Issues 1-2, July 2004, Pages 97-107.

37. G. Bagheri, S.E. Hosseini, and M.A. Wahid. Effects of bluff body shape on the flame stability in premixed micro-combustion of hydrogen-air mixture. Applied Thermal Engineering, Volume 67, Issues 1-2, 2014, Pages 266-272.

38. M. Akram and S. Kumar. Experimental studies on dynamics of methane-air premixed flame in meso-scale diverging channels. *Combustion and Flame*, Volume 158, Issues 5, 2011, Pages 915-924.

39. Y. Yan, W. Huang, W. Tang, L. Zhang, L. Li, J. Ran, and Z. Yang. Numerical study on catalytic combustion and extinction characteristics of pre-mixed methane-air in micro flatbed channel under different parameters of operation and wall. *Fuel*, Volume 180, 2016, Pages 659-667.